DOI: 10.1002/fuce.201300217

Fuel Cells

ORIGINAL RESEARCH PAPER

Signal Processing and Stochastic Filtering for EIS Based PHM of Fuel Cell Systems▲

M. Gašperin[1]*, P. Boškoski[1], A. Debenjak[1], J. Petrovčič[1,2]

[1] Department of Systems and Control, Jožef Stefan Institute, Jamova 39, Ljubljana SI-1000, Slovenia
[2] CO NOT, Hajdrihova 19, Ljubljana, Slovenia

Received: September 30, 2013; accepted: April 12, 2014; published online June 03, 2014

Abstract

This paper presents an alternative computational method for on-line estimation and tracking of the impedance of PEM fuel cell systems. The method is developed in order to provide the information to diagnostics and health management system. Proper water management remains the main issue influencing the reliability and durability of PEM fuel cell technology. While literature reviews reveal the thorough understanding of the underlying processes and extensive experimental work, the existing implementations rely on expensive hardware or time consuming computational methods. In this scope, we will show how the characteristic values of the fuel cell impedance, required by the diagnostic system, can be computed by robust and computationally efficient algorithms, which are suitable for implementation in embedded systems. The methods under consideration include continuous-time wavelet transform (CWT) and extended Kalman filter (EKF). The CWT is a time-frequency technique, which is suitable for tracking transient signal components. The EKF is a stochastic signal processing method, which provides confidence measures for the estimates. The paper shows, that both methods provide accurate estimates for diagnostics of FCS and can perform on-line tracking of these features. The performance of the algorithms is validated on experimental data from a commercial fuel cell stack.

Keywords: Electrochemical Impedance Spectroscopy, Fuel Cell Diagnostics, Non-linear Kalman Filter, Prognostics and Health Management

1 Introduction

Proton Exchange Membrane (PEM) fuel cells experience reliability issues due to water management faults [1]. On the one hand, when produced water is not effectively removed from the cell, flooding of gas-diffusion layer occurs, while excessive water removal leads to membrane drying, on the other hand. Both faults negatively affect performance of PEM fuel cells, and therefore have to be properly handled in order to ensure long-term reliability of PEM fuel cell operation.

A number of research projects and experimental work showed that implementation of Prognostics and Health management (PHM) methodologies may significantly contributes to the overall reliability and durability of Fuel Cell Systems (FCS) [2–6]. This paper follows the idea to use the Electrochemical Impedance Spectroscopy (EIS) as a diagnostic parameter. Its effectiveness has already been proven on laboratory-scale FCS, [7]. The estimation of a FCS model trough the EIS was used to distingush a nomal operating cell from flooded or dried [8, 9] and to estimate the aging time [10]. Additionally, authors report they can detect anode catalist carbon monoxide poisoning [11]. Recently [12] presented a high-voltage impedance spectrometer for testing multi-cell stacks. While demonstrating good diagnostics performance, the measurement equipement used in most studies is prohibitely expensive for commercial applications and one often encounters several other difficulties arising mainly from data acquisition, signal processing and computational requirements.

The common theme in the majority of the reported research is that they aim to directly implement the methodology from the laboratory devices into the commercial applications. The methods rely on the application of Fourier transform to compute the impedance at different excitations signals. When the operating conditions are stable and the cell is operating in stationary regime, this approach provides an

▲ *Paper presented at the "Fundamentals & Developments of Fuel Cells Conference 2013 (FDFC2013)", April 16–18, 2013, Karlsruhe, Germany.*

[*] *Corresponding author, matej.gasperin@ijs.si*

accurate image of the impedance spectrum. However, such implementation results in an unwanted increase in complexity of the fuel cell system. Furthermore, the reliability and robustness of these implementations in real-world applications has not yet been validated.

The aim of this paper is to present two novel approaches for computational estimation of the impedance characteristic of the FCS. They proposed methods are based on stochastic signal processing and Bayesian state estimation. While both approaches result in algorithms with sufficient diagnostic accuracy, the distinct properties might make them more appropriate for different applications.

Spectral analysis of signals is one of the most common signal processing techniques. The most widely used spectral analysis approach is the Fourier transform. However, such an approach results into a time averaged view of the present spectral components and their properties. As a result, the application of Fourier transform can obscure some transient signal components [2]. One way to overcome these limitations is the application of time-frequency signal processing techniques, such as the wavelet transform. Therefore, the FCS impedance was estimated by performing continuous wavelet transform of the corresponding electrical signals using the complex Morlet wavelet. Such a transform results into a set of complex wavelet coefficients that preserve information about the amplitude and instantaneous phase of the signal's components.

As an alternative to the most commonly used based implementation, we investigate an approach based on stochastic filtering. An example of this class of algorithms was investigated in [13], where authors used real-time observers. The approach overcomes the computational issues because it is based on less demanding methods. At the same, such algorithms can cope with non-stationary stochastic components of the signals and measurement uncertainties. For this we propose a mathematical representation of the FCS impedance in the form of a state-space model. We show that using this model formulation, it is possible to consistently estimate the characteristic values of the FCS impedance at different frequencies. Estimation of the model state variables is performed with Extended Kalman Filter (EKF), which is renowned for its computational efficiency. The main difference to related model-based methods, such as the one presented in [14] is that they still rely on AC impedance measures and transformation of signals to frequency domain. It is important to stress that the presented method completely avoids the need for such transformation.

The main advantages of the proposed implementation are computational efficiency and probabilistic interpretation of the results. Computational load of the EKF algorithm is low, due to the inherent recursive nature of the Kalman filter, which in turn greatly simplifies the computation. The algorithm is also based on Bayesian probability theory, which means that all the estimates are given in the form of probability density functions, which ensures adequate management of the uncertainties. The validation of the algorithms is performed on experimental data, recorded on 8.5 kW PEM FCS using a special purpose measurement system. The results demonstrate that the estimates impedance is accurate enough to distinguish between different operating regimes using only a limited number of impedance features.

2 Background: Modeling the Impedance of Fuel Cell Systems

The impedance is defined as a ratio of the voltage phasor to the electric current phasor. To estimate its value, given two sampled waveforms, one usually computes the phasors in frequency domain and the impedance is given by their ratio. In the specific case of FCS impedance estimation, there are some important properties that are often ignored [2,4] (i) in case of sinusoidal current excitation, the voltage will have the same sinusoidal form corrupted by random noise, (ii) the signals (both voltage and electric current) contain only one frequency component, (iii) the frequency of the component is known and is the same for both signals. Taking into account the above, we can model both signals as:

$$i(t) = I\cos(\omega t + \phi_i) + e_i(t), \tag{1}$$

$$u(t) = U\cos(\omega t + \phi_u) + e_u(t), \tag{2}$$

where we can ignore the DC component of the signals without the loss of generality. Assuming known frequency ω, both signals are fully specified by their amplitude and phase. The complex phasors are:

$$I = Ie^{j\phi i} + e_i, \tag{3}$$

$$U = Ue^{j\phi u} + e_u. \tag{4}$$

And finally the complex impedance is defined by their ratio:

$$Z = \frac{U}{1} = \frac{U}{I}e^{j(\phi_u - \phi_i)} + e_z. \tag{5}$$

It is important to note, that given this representation, the only quantities required are the amplitudes (I, U) and phase angles (ϕ_i, ϕ_u). For automatic estimation of the signals, we describe the time evolution of the parameters with a state-space model. In this implementation, the hidden system states are the amplitude and phase $x_k = (I, \phi_i)^T$, which follow the random walk model and thus have the following state transition equation:

$$x_{k+1} = \begin{bmatrix} 1 & 0 \\ 0 & 1 \end{bmatrix} x_k + v_k, \tag{6}$$

The measured output is the sinusoidal waveform (7).

$$y_k = I\cos(\omega T_s k + \phi_i) + e_k = x_k(1)\cos(\omega T_s k + x_k(2)) + e_k, \tag{7}$$

where k is sample index, x_k is the hidden system state, y_k is the model output, T_s is the sampling interval, and ω is the angular frequency. With proper selection of system states and assuming a time-invariant and known frequency ω, the presented equations can model any sinusoidal waveform with-

out a DC component. The DC component can either be removed in pre-processing or included is the model. For the sake of clarity we will assume that all the signals are without a DC component.

Derivation and the result for the voltage signal is exactly the same as for electric current and will be skipped for the sake of brevity. Both models are merged to one model with four states and two outputs.

3 EKF Based Algorithm for On-line Impedance Tracking

The task of estimation can be interpreted as a problem of inference of a discrete-time stochastic process:

$$y_k \sim p(y_k|x_k), \tag{8}$$

$$x_k \sim p(x_k|x_{k-1}). \tag{9}$$

Here, x_k is a vector known as the state variable, y_k are the observations, and $p(\cdot|\cdot)$ denotes the conditional probability density of the variable. By Bayesian state estimation we mean the recursive evaluation of the filtering distribution, $p(x_k|y_{1:k})$, using Bayes rule [18]:

$$p(x_k|y_{1:k}) = \frac{p(y_k|x_k)p(x_k|y_{1:k-1})}{p(y_k|y_{1:k-1})}, \tag{10}$$

$$p(x_k|y_{1:t-1}) = \int p(x_k|x_{k-1})p(x_{k-1}|y_{1:k-1})dx_{k-1}, \tag{11}$$

where $y_{1:k} = (y_1, y_2, \ldots y_k)$ denotes the set of all observations. The integration in (11) is over the whole support of the involved probability density functions. Eqs. (10) and (11) are analytically traceable only for a limited set of models. The most notable example of a traceable model is linear Gaussian model for which (10) and (11) are equivalent to the Kalman filter. For other models, operations (10)–(11) do not yield posterior density in the form of a Gaussian and they need to be evaluated approximately. One possible method is the Extended Kalman filter [19], which assumes that probability densities in (8) and (9) are:

$$p(x_k|x_{k-1}) = N(g(x_{k-1}), Q), \tag{12}$$

$$p(y_k|x_k) = N(h(x_k), R), \tag{13}$$

where g(·) and $h(\cdot)$ are vector functions of appropriate dimensions, $N(\cdot,\cdot)$ denotes Gaussian probability density. Finally, Q and R are covariance matrices for process and measurement noises, respectively. Using Taylor expansion at the current point estimate as follows:

$$p(x_k|x_{k-1}, y_{1:k-1}) \approx \tilde{N}(g(\hat{x}_{k-1}), P_t), \tag{14}$$

$$p(x_k|x_{k-1}, y_{1:k}) \approx N(g(\hat{x}_{k-1}) - K(y_k - g(\hat{x}_{k-1})), P_{k|k}), \tag{15}$$

where K and P_k are the Kalman gain and posterior covariance matrix from the Kalman filter.

$$S = C^T P_{k-1} C + R \tag{16}$$

$$K = P_{k-1} C S^{-1} \tag{17}$$

$$P_{k|k} = P_{k-1} - P_{k-1} C^T S^{-1} C P_{k-1} \tag{18}$$

$$P_k = A P_{k|k} A^T + Q \tag{19}$$

where $A = (d/\mathrm{d}x_k)g(x_k)$ and $C = (d/\mathrm{d}x_k)h(x_k)$ [18]. This approximation is performed in each step. The applied algorithm for impedance tracking in FCS was designed by implementing the presented solutions in the final version of the algorithm. A single iteration of the estimation algorithm for a single cell in the stack is summarized in Table 1.

The key advantages of the algorithm, namely the proper management of uncertainty and recursive implementation, are both inherited from the EKF. Another desired property is, that the impedance is not assumed to be constant (as opposed to FFT-based implementations, where non-stationary signals actually cripple the estimation) and the algorithm recursively estimates its current value. Finally, the EKF retains the low computational complexity of the linear Kalman filter, which makes it an appropriate choice for advanced applications of diagnostic tools in FCS (i.e., on-board monitoring of individual cell impedance).

4 Impedance estimation with Continues Wavelet Transform

The application of Fourier transform is suitable for regular signals (roughly stated smooth periodic signals). However for signals describing transient phenomena, located in a narrow time interval, the application of Fourier transform turns to be inadequate. With properly tuned CWT parameters, this approach provides reliable impedance results along the entire frequency band. The wavelet transform is widely used tool in a variety of scientific fields. In the area of PEM fuel cell diagnostics, Steiner et al. [15] used discrete wavelet transform to diagnose PEM fuel cell flooding directly from the voltage signals.

The flooding was diagnosed based on the pattern of the wavelet packet coefficients derived with the wavelet packet transform.

Wavelet transform is based on a setof specifically designed functions called wavelets. The continuous wavelet transform (CWT) of a square integrable function $f(t) \in \boldsymbol{L}^2(\mathbb{R})$ is defined as [16, 17]:

Table 1 EKF based algorithm for impedance estimation.

	Algorithm: On-line tracking of FCS impedance with EKF
1	Start with initial estimates of voltage and current waveforms I_0, $\phi_{i,0}$, U_0, $\phi_{u,0}$ and set the sampling period T_s
2	for k = 1:N
3	Collect new samples of U_k and I_k
4	Compute the EKF estimate of states I_k and $\phi_{i,k}$ (16)
5	Compute the EKF estimate of states U_k and $\phi_{u,k}$ (16)
6	Compute the FCS impedance Z_k (5)
7	end for

$$W_f(a,b) = \langle f(t), \psi_{a,b}(t) \rangle = \int_{-\infty}^{\infty} f(t)\psi_{a,b}(t)\,\mathrm{d}t, \tag{20}$$

where $\psi_{a,b}(t)$ is a version of the mother wavelet $\psi(t)$ translated by a and dilated by b:

$$\psi_{a,b}(t) = \frac{1}{\sqrt{a}}\psi\left(\frac{t-b}{a}\right). \tag{21}$$

The CWT transform (20) describes the analyzed signal $f(t)$ on the time–frequency plane. The conversion between scale s and actual frequency f is straightforward and depends on the selection of the mother wavelet (21). Each scaling s alters the time–frequency resolution of the mother wavelet. As a result, CWT offers adaptive time–frequency resolution. High frequency resolution is preserved for lower frequencies, whereas high time resolution is preserved for higher frequencies [16].

For impedance estimation, one needs information about the instantaneous amplitude and phase of the electrical current $i(t)$ and voltage $u(t)$. Therefore, a logical choice for mother wavelet (21) is the complex Morlet wavelet. In the time domain the complex Morlet wavelet is a sine signal modulated by a Gaussian window as:

$$\psi(t) = \sqrt{2}\mathrm{e}^{-t^2/a^2}(\mathrm{e}^{j\pi t} - \mathrm{e}^{-\pi^2 a^2/4}). \tag{22}$$

The Fourier transform of (3) is:

$$\mathcal{F}\{\psi(t)\} = \hat{\psi}(\omega) = \frac{a\mathrm{e}^{-a^2}(\pi^2+\omega^2)}{4(\mathrm{e}^{\pi a^2\omega/2}-1)}. \tag{23}$$

Consequently, the wavelet coefficients $W_f(a,b)$ in (1) are complex values. As a result, at each time translation a and scale b, the CWT with Morlet wavelet provides value of the instantaneous amplitude and phase.

4.1 Impedance Calculation Using CWT

The impedance of the FCS is calculated through the coefficients of the CWT. By using the Morlet wavelet, one calculates the wavelet coefficients of both $u(t)$ and $i(t)$. Since the resulting wavelet coefficients are complex, each of them describes the instantaneous amplitude and phase of both signals over the selected frequency range, specified by the range of scales b for each time moment t in (20). The instantaneous impedance for each frequency is then calculated as a ratio between the corresponding wavelet coefficients as:

$$Z(u) = \left.\frac{W_u(a,b)}{W_i(a,b)}\right|_{b=\omega} \tag{24}$$

where W_u (a, b) and W_i (a, b) are the CWT coefficients of $u(t)$ and $i(t)$ respectfully. The number of wavelet coefficients for specific scale s corresponds to the number of acquired measurements.

4.2 Cone of Influence

Due to the finite length of the signals at hand, the values of some of the wavelet coefficients are influenced by the abrupt signal edges. These discontinuities introduce false broad frequency components whose influence varies over different wavelet scales. This effect defines the so-called cone of influence.

The shape of the cone of influence depends on the mother wavelet $\psi(t)$. For the Morlet wavelet this region is shown as hatched area in Figure 1. The coefficients in the selected area should be omitted from further analysis. In Figure 1, it can be noticed that all of the low frequency wavelet coefficients are influenced by the discontinuities occurring on both edges. One can overcome this limitation by either using longer signal or by oversampling the existing one.

5 Experimental Setup and Results

To obtain realistic data, the measurements were performed by the Fuel Cell Voltage Monitor (FCVM), which is an embedded signal acquisition module, designed for accurate measurement of voltage signals of FCS. The FCVM enables measurements of the voltage of individual cell inside the stack.

The analysis of the experimental data is aimed at demonstrating the performance of two alternative algorithms for estimation of FCS impedance on commercial device. The proposed algorithms require minimum hardware and software specifications and are able to operate in non-stationary conditions and under uncertainty in the measurements. Let us note that for the purpose of FCS diagnostics, the characterization of the entire impedance spectrum is not required. The aim of the methods is only to detect the sufficient change at the characteristic frequencies and this section is organized accordingly.

5.1 Fuel Cell Voltage Monitor

When it comes to commercially oriented applications, the measurement equipment needs to be capable of measuring voltages of all individual cells inside a FCS, rather than measuring only a single cell or a stack of few cells in the case of

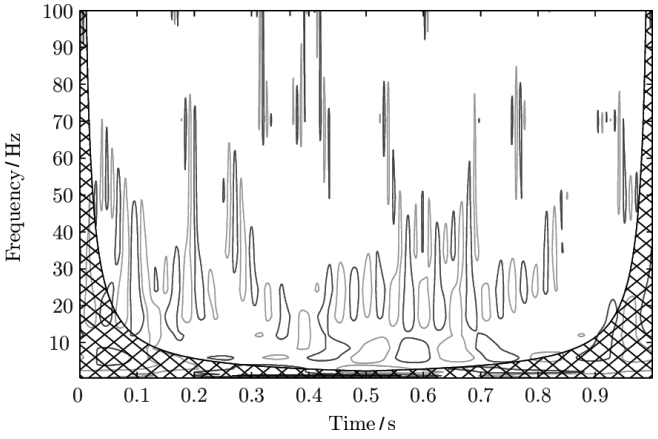

Fig. 1 Cone of influence for the Morlet wavelet.

laboratory testing [20]. State-of-the-art laboratory equipment and data acquisition boards can successfully cope with the measurement requirements, but their design solutions and measurement concepts are not appropriate for commercial applications, primarily because of high costs. Additionally, target requirements regarding reliability, size, and weight for such commercial equipment are much stricter than for the laboratory-grade one [20]. To fulfill the requirements, the manufacturers use design solutions that measure joint voltage of two or even more adjacent cells with rather low resolution. The developed Fuel Cell Voltage Monitor (FCVM), presented in Figure 2, overrides earlier discussed shortcomings of nowadays measurement solutions for commercial applications. In its essence, the FCVM is a low-cost general-purpose device, designed for accurate measurement of voltage signals of FCS consisted of up to 90 FCs.

The main problem with measuring individual cell voltage inside a large stack is mainly connected with common-mode (C-M) voltage potential, which is the origin of high complexity and costs of the laboratory-grade equipment. Typically, commercial PEM FCS embodies 50–100 cells resulting in open-circuit voltage of 60–120 V. Such high C-M potential prohibits usage of integrated-circuit multiplexors in a standard way. To override this limitation, the FCVM's analog input stage for the cell voltages is designed around three pairs of multiplexors, each coupled with a differential amplifier, which eject C-M voltage and change the differential signals to ground referenced single-ended ones in order to fit to the AD converter.

The main feature of the FCVM is the ability to perform measurements intended for more complex diagnostics tools. The EIS based diagnostics relies on precise measurements of FCS voltage and current, which must exhibit high resolution, and must be carried out at high sampling rate. Both, high resolution and sampling rate are required because of the superimposed AC voltage signals, which are to be measured, and their low amplitude not higher than few millivolts and frequencies ranging up to few hundred Hertz. As such, the FCVM provides the means for EIS diagnostics. It enables measuring changes in voltage of specific cell inside a stack with resolution of ~80 μV at high sampling rate. More precisely, the FCVM enables simultaneous measurements of three cells voltages at sampling rate of 5 kHz. Beside the individual cells voltages, voltage and current of the complete stack are also measured at the same sampling rate, and with a resolution of ~24 mV and ~10 mA, respectively. To measure all 90 cells, the measurements are performed in interlaced manner in 30 consecutive time periods. Besides providing the measurement capacities, the FCVM was built to be on-line EIS-based diagnostic module with its own computation resources provided by on-board ARM Cortex M3 based microcontroller.

The measurement setup consisted of a commercial 8.5 kW PEM fuel cell power unit, electronic load, FCVM measuring system, and the PC. The unit was connected to an electronic load, which served to provide the excitation current. The FCVM and desktop computer formed the data acquisition subsystem of the measurement setup.

5.2 Experimental Protocol

Based on the previous research [21], the systems response was observed at the frequencies 10, 30, and 100 Hz. During the experiment, the current's DC component was set to 40 A, and the amplitude of the single frequency sinusoidal current excitation was set to 1 A. Figure 3 shows the FCS used for the experiment.

The experimental data includes a simulated fault scenario, where the power unit was fed with different input gases, while all other operational parameters were kept constant. Due to practical reasons, the experiment was designed to only simulate cell flooding.

The experiment went through three stages: normal, flooded, and back to normal stage. Throughout the experiment, five parameters were constantly monitored: stack voltage, stack current, and voltage of three single cells in the FC. In the first time period, the power unit operated on normal ambient air with temperature 50 °C and relative humidity of 12%. The first phase lasted for approximately 50 min. Then the system was fed with saturated air with temperature 50 °C and relative humidity of 100% for 1 h. Finally, the power unit again operated under normal conditions. The measurement of individual cell is performed every 40 sand records 1 s of the signal. This signal length is adequate to ensure the con-

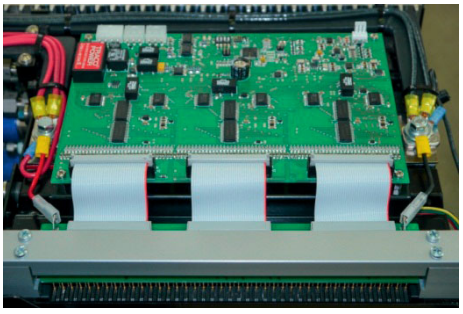

Fig. 2 Fuel Cell Voltage Monitor (FCVM) voltage monitor connected to the stack.

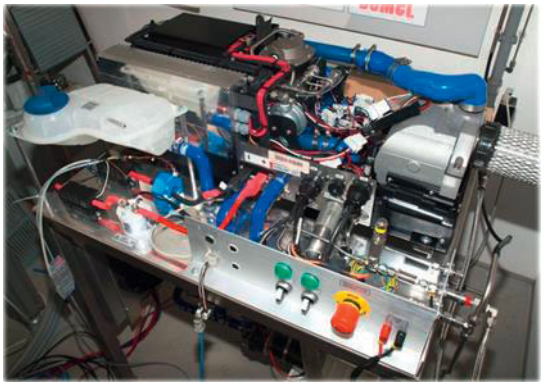

Fig. 3 8.5 kW PEM Fuel Cell power unit.

vergence of the proposed algorithms for excitation signals with the frequencies higher than 10 Hz. The duration of the experiment was 8000 s (approximately 2 h).

5.3 CWT Impedance Tracking Results

The acquired signals were analyzed using continuous wavelet transform with complex Morlet mother wavelet. As the frequency of the superimposed single component signal is known in advance, the impedance was estimated by using the complex wavelet coefficients for the specified frequency. The instantaneous values of the FCS impedance are calculated as a ratio between the complex wavelet coefficients of the cell voltage $u(t)$ and its current $i(t)$. The calculation process includes only the wavelet coefficients from the cone of influence which minimizes the edge influence.

The results for particular frequency of the superimposed signal are shown in Figures 4–6. The different shaded regions represent different operating regimes, where in the white region (0–3,000 s) the cell is fed with normal air and in the blue region (3,000–7,000 s) it is fed with moisture saturated air. For each measurement section, we have estimated the mean (black line) and the variance (shaded area) of the wavelet coefficient for specific scale (frequency) b.

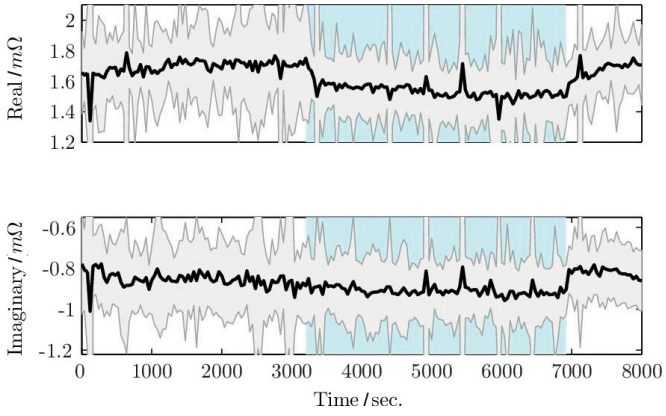

Fig. 4 Impedance estimation from CWT algorithm at the excitation signal with frequency 10 Hz.

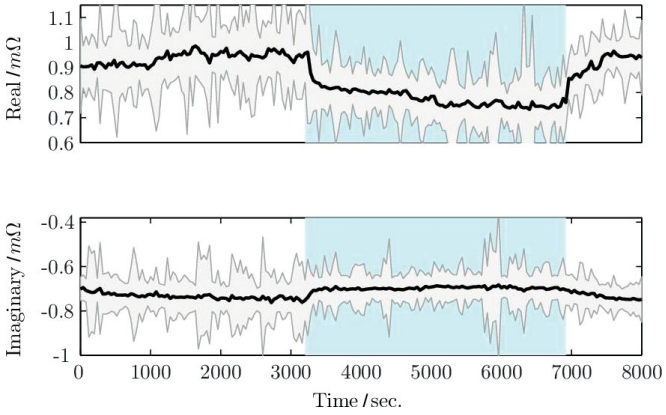

Fig. 5 Impedance estimation from CWT algorithm at the excitation signal with frequency 30 Hz.

The changes in the humidity condition of the FCS visibly alter the impedance of the cells. The flooding segment lasted in the interval [3,000, 7,000] s. It can be noticed that the flooding causes certain drop in the resistance and increase of the reactance. This effect is mostly visible for the signals that have superimposed perturbations with the frequency 100 Hz. On the other hand, the signal with lower frequency components, exhibit minor impedance changes.

5.4 EKF Impedance Tracking Results

The second implementation of on-line tracking of the cell impedance is achieved by the Extended Kalman filter algorithm, given in Table 1. The excerpt of the estimation procedure for a single cell at a single measurement sample, where the excitation signal with frequency 10 Hz was used is given in Figure 7. The left part of the images shows the tracking of the waveform parameters in terms of mean (bold) and confidence interval (shaded) and the right part shows the estimated impedance value, where the size of the marker corresponds to the uncertainty interval. This estimation is then performed for each measurement sample.

It can be seen that the algorithm converges in about 200 samples, which correspond to four periods of the excitation signal. After this number of samples, the confidence interval of the estimate narrows down considerably. As the computation of the Kalman filter involves only computationally undemanding numerical operations, the execution of the algorithm is extremely fast. Second distinct advantage is the recursive nature of the algorithm.

The EKF estimation from Figure 7 is performed for each measurement sample, where the initial estimate for the next sample is set to the final estimate of the previous one. This initialization additionally speeds up the convergence. The resulting trajectories for the different frequencies are shown in Figures 8–10. The different shaded regions represent different operating regimes, where in the white region (0–3,000 s) the cell is fed with normal air and in the blue region (3,000–7,000 s) it is fed with moisture saturated air.

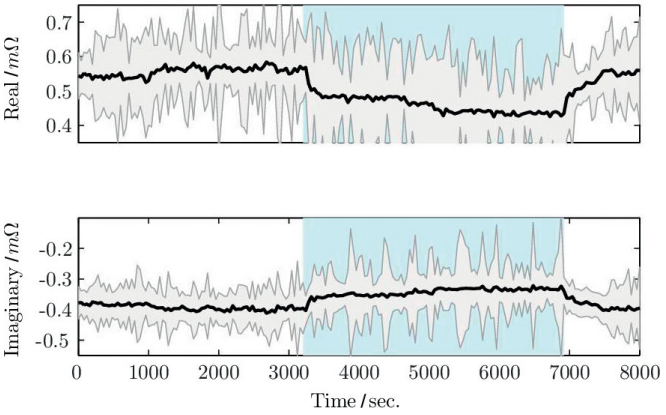

Fig. 6 Impedance estimation from CWT algorithm at the excitation signal with frequency 100 Hz.

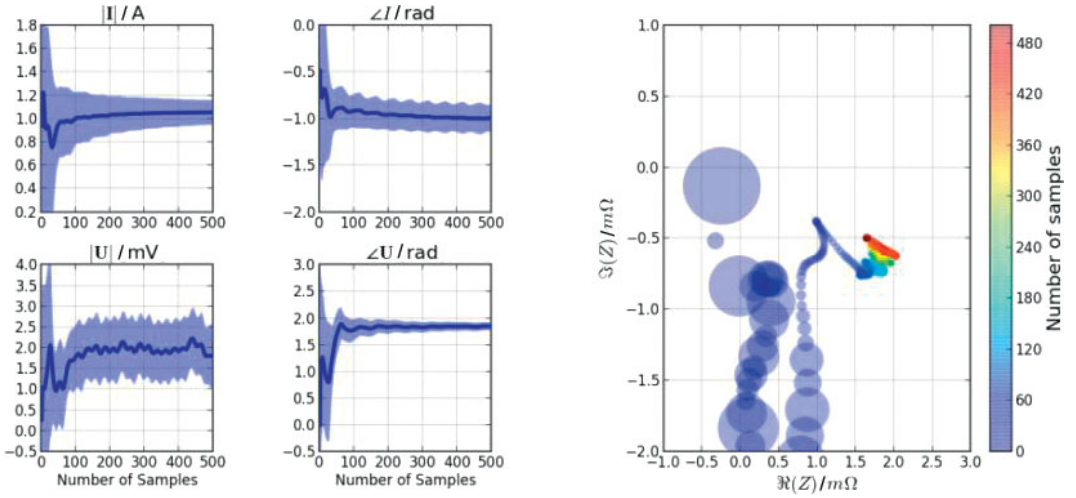

Fig. 7 Estimates of the electric current and voltage signals (left) and cell impedance (right), computed at 10 Hz signal frequency and 500 Hz sampling frequency using 500 samples.

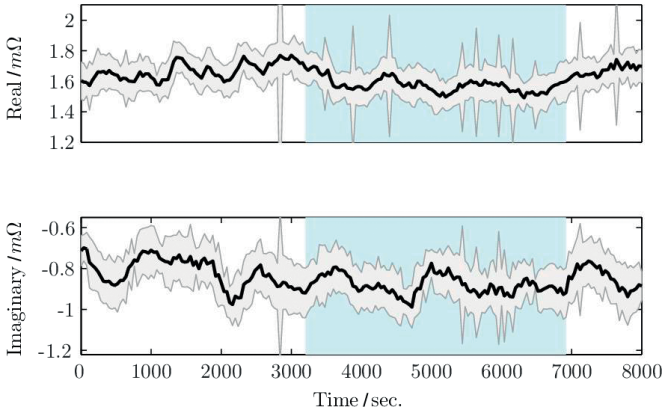

Fig. 8 Impedance tracking with EKF algorithm at the excitation signal with frequency 10 Hz.

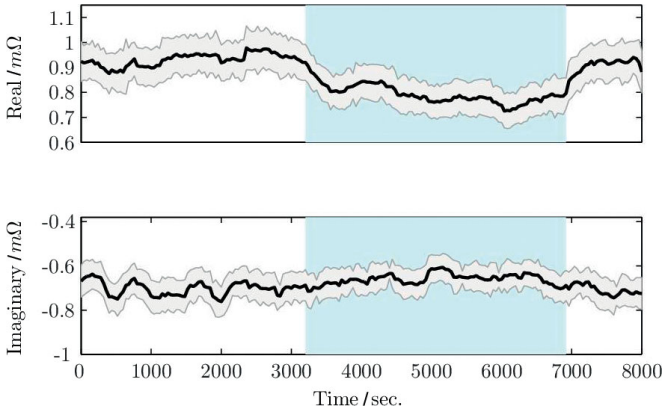

Fig. 9 Impedance tracking with EKF algorithm at the excitation signal with frequency 30 Hz.

Black line represents the mean value of the estimate and the shaded area corresponds to 95% confidence interval.

It can be seen that compared to the CWT, the results show lower resolution and the change in the system impedance with the presence of moist air is not as distinct. However, the drop in the real component is still sufficient to separate and classify the two different regimes.

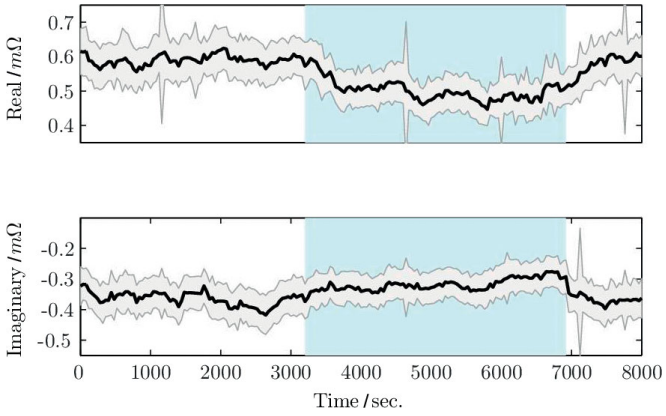

Fig. 10 Impedance tracking with EKF algorithm at the excitation signal with frequency 100 Hz.

It is important to stress, that the selection of the noise covariance matrices Q and R is an important tuning parameter with the Kalman filtering framework. In general, lower values of covariance matrices result in slower convergence, while higher values result in erratic estimates. Therefore, by tuning of these matrices, one can adjust the sensitivity and confidence in the estimates, which can make the diagnostic algorithm more conservative or confident in the estimate.

The probability density function of the initial value for the estimate is another tuning parameter, which has to be determined experimentally (e.g., by off-line analysis). Due to the favorable properties of the Kalman filtering framework, the algorithm is not very sensitive to the selection as long as the initial estimates are reasonably close to the actual values.

6 Conclusion

The Fuel Cell PHM system consists of several subcomponents, including data acquisition, processing, decision mak-

ing etc. In this paper, we focus on only one of these modules, namely the signal processing. The input to the presented algorithms is the current and voltage signals from the FCS and the output is the estimated impedance. In the context of the PHM system, these impedance values are used by the reasoning module to determine the type and extent of the fault.

The results indicate that successful on-board EIS based diagnostics of FCS can be achieved using relatively simple and inexpensive measurement equipment and optimized computational procedure. We consider two possible numerical estimation procedures that can replace the special purpose EIS measurement devices.

First candidate is the continuous wavelet transformation, which operates in time-frequency domain and provides fast and reliable estimates of the instantaneous impedance, without the strong limitations on the signal stationary. Furthermore, the analysis of the signals with CWT has shown that the recorded voltage and current signals may be heavily corrupted by noise, either resulting from the measurement process or inherent random nature of the FCS. When considering application of the PHM techniques to commercial systems, the lack of proper management of the uncertainty can lead to an increased number of miss-diagnosed faults and possible equipment failures. Therefore, the algorithms that can operate in under these assumptions have to be employed.

Second option for on-line impedance tracking is implementation of stochastic Bayesian filtering methods. The presented algorithm relies on the simple model of a voltage and current waveforms. The impedance is estimated from the parameters of the waveforms, which are estimated on-line by the Extended Kalman filter. This implementation is computationally efficient as the computation involves simple matrix operations, fully recursive and can properly manage the noise components in the measurements.

The motivation in development of the methods was to design robust and computationally efficient methods that can determine the change in fuel cell health. Therefore, the estimated impedance values do not necessarily represent the "true" impedance, but can also include effects of the measurement and signal processing procedures. Furthermore, the latter ones are algorithm specific, which leads to slightly different estimated values on the same data. In the current implementation, both methods are meant to be used solely for diagnostic purposed and not for exact physical or chemical modeling the fuel cell.

Future work in the development of the diagnostics and health management system for FCS will be to investigate different models of the FCS operation with respect to water content and other anticipated faults. The use of parametric models, such as electric circuits, with proper model parameterization will improve the quality of the estimates and provide better information to the diagnostic decision making algorithm. Furthermore, general structure of the Kalman filtering framework allows high flexibility in terms of possible model structures and excitation signals, which can be determined so that the estimation will require minimum execution time and perturbation of the cell.

Acknowledgements

This work was supported by the Slovenian Research Agency through grant Z2-5477 and the Centre of Excellence for Low-carbon Technologies – CO NOT, financed by the Slovenian Ministry of Higher Education, Science and Technology and co-financed by the European Regional Development Fund.

References

[1] W. Schmittinger, A. Vahidi, *J. Power Sources* **2008**, *180*, 1.
[2] S. M. R. Niya, M. Hoorfar, *J. Power Sources* **2013**, *240*, 281.
[3] Z. Zheng, R. Petrone, M. Péra, D. Hissel, M. Becherif, C. Pianese, N. Y. Steiner, M. Sorrentino, *Int. J. Hydrogen Energ.* **2013**, *38*, 8914.
[4] F. A. de Bruijn, V. A. T. Dam, G. J. M. Janssen, *Fuel Cells* **2008**, *8*, 3.
[5] R. Petrone, Z. Zheng, D. Hissel, M. Péra, C. Pianese, M. Sorrentino, M. Becherif, N. Y. *Int. J. Hydrogen Energ.* **2013**, *38*, 7077.
[6] J.-M. L. Canut, R. M. Abouatallah, D. A. Harrington, *J. Electrochem. Soc.* **2006,** *153*, 857.
[7] K. P. Adzakpa, K. Agbossou, Y. Dube, M. Dostie, M. Fournier, A. Poulin, *IEEE Trans. Energy Conver.* **2008,** *23*, 581.
[8] H. Li, Y. Tang, Z. Wang, Z. Shi, S. Wu, D. Song, J. Zhang, K. Fatih, J. Zhang, H. Wang, Z. Liu, R. Abouatallah and A. Mazza, *J. Power Sources* **2008,** *178*,103.
[9] A. Forrai, H. Funato, Y. Yanagita, Y. Kato, *IEEE Trans. Energy Conver.*, **2005**, *20*, 668.
[10] R. Onanena, L. Oukhellou, D. Candusso, F. Harel, D. Hissel, P. Aknin, *International J. Hydrogen Energ.* **2011**, *36*, 1730.
[11] X. Yuan, H. Wang, J. C. Sun, J. Zhang, *Int. J. Hydrogen Energ.* **2007**, *32*, 4365.
[12] S. Wasterlain, D. Candusso, F. Harel, D. Hissel, X. François, *J. Power Sources* **2011**, *196*, 5325.
[13] B. Nahid-Mobarakeh, M. Hinaje, B. Davat, *Proc. 5th International Conference on Fundamentals & Development of Fuel Cells*, Karlsruhe, Germany, **2013**.
[14] N. Fouquet, C. Doulet, C. Nouillant, G. Dauphin-Tanguy, B. Ould-Bouamama, *J. Power Sources* **2005**, *159*, 905.
[15] N. Y. Steiner, D. Hissel, P. Moçotéguy, D. Candusso, *Int. J. Hydrogen Energ.*, **2011**, *36* 740.
[16] S. Mallat, *A Wavelet Tour of Signal Processing*, Elsevier Academic Press, Burlington, MA, USA, **2008**.
[17] P. S. Addison, *Physiol. Meas.* **2005**, *26*, 155.
[18] D. Simon, *Optimal State Estimation*, John Wiley & Sons, Hoboken, NJ, USA, **2006**.

[19] S. Haykin, (Ed.) *Kalman Filtering and Neural Network,* John Wiley & Sons, New York, USA, **2001**.
[20] M. Miller, A. Bazylak, *J. Power Sources* **2011**, 196, 601.
[21] D. Webb, S. Moeller-Holst, *J. Power Sources* **2001**, *103*, 54.
[22] A. Debenjak, M. Gašperin, B. Pregelj, M. Atanasijevixč-Kunc, J. Petrovčič, V. Jovan, *Strojniški vestnik – J. Mech. Eng.* **2013**, *59*, 56.

